Easy Tuning of PID Controllers for Specified Performance

Š. Bucz*, A. Kozáková* and V. Veselý*

*Institute of Control and Industrial Informatics,
Faculty of Electrical Engineering and Information Technology,
Slovak University of Technology in Bratislava, Ilkovičova 3, SK-812 19 Bratislava, Slovak Republic
(e-mail: stefan.bucz@stuba.sk, alena.kozakova@stuba.sk, vojtech.vesely@stuba.sk)

Abstract: The presented method allows achieving maximum overshoot and specified settling time of the closed-loop step response. It provides a simple way to control linear stable SISO systems even if the mathematical model is unknown. Tuning rule parameters are based on one suitably chosen point of the plant frequency response obtained by sine-wave signal with specified excitation frequency, and the required phase margin. The main result provided is construction of empirical charts used to convert time-domain performance specifications (maximum overshoot and settling time) into frequency domain performance measure (phase margin). The method is applicable for systematic shaping of the closed-loop response of the plant. The new approach has been verified on a set of benchmark examples and on a real plant as well.

Keywords: PID controller, performance assessment, overshoot, settling time, phase margin, gain crossover

1. INTRODUCTION

Tuning methods are typically two-stage procedures consisting of identification of certain characteristic data of the plant with unknown mathematical model, followed by controller design. Controller tuning rules that directly include identified plant data have been developed experimentally by technological process specialists (Veselý, 2003). The widespread use of their modern versions is due to their simple implementation and possibility to directly integrate performance specifications into controller design algorithms. Although there are about 408 various sources of PID controller tuning methods (Åström and Hägglund, 2000), 30% of implemented controllers permanently operate in manual mode, and 25% of them use factory-tuning without any up-date with respect to the specific plant. Hence, there is natural need for effective PID controller design algorithms that enable not only modifying the controlled variable but also achieving specified performance (Kozáková et al., 2010), (Osuský et al., 2010).

Main advantage of the proposed PID tuning method is a fast design procedure for performance specified in terms of maximum overshoot η_{max} and settling time t_s, with no need for exact mathematical model of the plant. Identification of characteristic data of the black-box type plant is carried out using sinusoidal excitation signal. The sine-wave engineering method enables to achieve

- $\eta_{max} \in \langle 0\%, 90\% \rangle$ and $t_s \in \langle 6{,}5/\omega_c, 45/\omega_c \rangle$ for plants with no integration behaviour,
- $\eta_{max} \in \langle 9.5\%, 90\% \rangle$ and $t_s \in \langle 11{,}5/\omega_c, 45/\omega_c \rangle$ for integrating plants (ω_c denotes critical frequency of the plant).

The paper is organized as follows: sine-wave identification technique is presented in Section 2, Section 3 describes the derived PID controller tuning rules based on guaranteed phase margin at a suitably chosen excitation frequency; achieved closed-loop performance is discussed in Section 4. The proposed method has been verified via simulation on benchmark examples, and on a real plant - a DC motor; the results are in Sections 5 and 6, respectively.

2. PLANT IDENTIFICATION BY A SINUSOIDAL EXCITATION INPUT

A setup for the proposed sine-wave method is in Fig.1, where *G(s)* is the transfer function of the plant with unknown mathematical model, and SW is a switch.

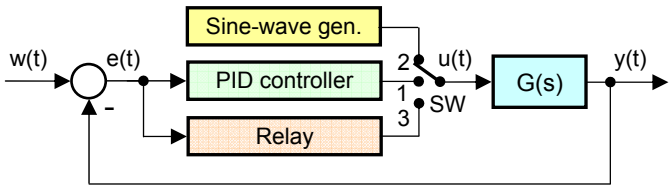

Fig.1. Multipurpose loop for the proposed sine-wave method

When the switch SW is in position „2“, a sinusoidal excitation signal with magnitude U_n and frequency ω_n (Fig.2a) is injected into the plant *G(s)*, i.e.

$$u(t) = U_n \sin(\omega_n t) \tag{1}$$

The plant output *y(t)* is also sinusoidal with the same frequency ω_n, magnitude Y_n and is the phase lag φ with respect to the excitation signal *u(t)* (Fig. 2b), i.e.

$$y(t) = Y_n \sin(\omega_n t + \varphi) \tag{2}$$

After reading the values Y_n a φ from the recorded values of *u(t)* and *y(t)*, a particular point of the plant frequency characteristics

$$G(j\omega_n) = |G(j\omega_n)| e^{j \arg G(\omega_n)} = [Y_n / U_n] e^{j\varphi(\omega_n)} \tag{3}$$

corresponding to the excitation frequency ω_n can be plotted in the complex plane (Fig.2c).

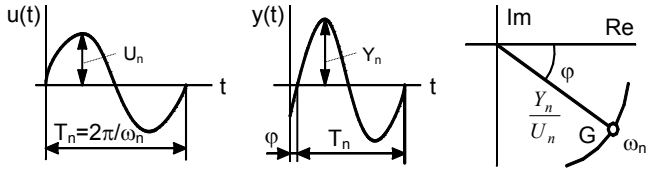

Fig.2. Time responses a) *u(t)*; b) *y(t)*; c) location of $G(j\omega_n)$ in the complex plane

The output sinusoid amplitude Y_n is affected by the excitation sinusoid amplitude U_n generated by the sine wave generator; it is recommended to choose $U_n=(3\div7)\%u_{max}$. Thus, identified plant parameters are represented by a triple $\{\omega_n, Y_n(j\omega_n)/U_n(j\omega_n), \varphi(\omega_n)\}$. With the SW in position „2", the identification is performed in open-loop, hence this approach is applicable for stable plants only. Excitation frequency ω_n is taken from empirically specified interval, and adjusted prior to identification (Bucz and Kozáková, 2012).

3. SINE-WAVE METHOD TUNING RULES

Consider the SW in Fig. 1 in position „1" and adjust the PID controller in manual mode ($G_R(s)$ is now a PID controller transfer function). The closed-loop characteristic equation $A(j\omega)=1+L(j\omega)=1+G(j\omega)G_R(j\omega)=0$ can be easily broken down into the magnitude and phase conditions

$$|G(j\omega_n)||G_R(j\omega_n)|=1 \tag{4}$$

$$arg\,G(\omega_n)+arg\,G_R(\omega_n)=-180°+\phi_M \tag{5}$$

where ϕ_M is required phase margin, $L(j\omega)$ is the open-loop transfer function. Graphical interpretation of (4), (5) is in Fig.3. Denote $\varphi=argG(\omega_n)$, $\Theta=argG_R(\omega_n)$, and consider the ideal PID controller in the form

$$G_R(s)=K\left[1+\frac{1}{T_i s}+T_d s\right] \tag{6}$$

where K is the proportional gain, and T_i, T_d are integral and derivative time constants, respectively. In the frequency-domain, comparison of the right-hand side of (6)

$$G_R(j\omega_n)=K+jK\left[T_d\omega_n-\frac{1}{T_i\omega_n}\right] \tag{7}$$

with the right-hand side of the PID controller in polar form

$$G_R(j\omega_n)=|G_R(j\omega_n)|e^{j\Theta}=|G_R(j\omega_n)|[\cos\Theta+j\sin\Theta] \tag{8}$$

yields a complex equality

$$K+jK\left[T_d\omega_n-\frac{1}{T_i\omega_n}\right]=\frac{\cos\Theta}{|G(j\omega_n)|}+j\frac{\sin\Theta}{|G(j\omega_n)|} \tag{9}$$

The PID controller parameters can be obtained from (8) and (9) using the substitution $|G_R(j\omega_n)|=1/|G(j\omega_n)|$ resulting from the magnitude condition (4). The complex equation (9) is then solved as a set of two real equations

$$K=\frac{\cos\Theta}{|G(j\omega_n)|} \tag{10a}$$

$$K\left[T_d\omega_n-\frac{1}{\beta T_d\omega_n}\right]=\frac{\sin\Theta}{|G(j\omega_n)|} \tag{10b}$$

where (10a) is a general rule for calculating the controller gain K; substituting (10a) and the ratio $\beta=T_i/T_d$ into (10b), a quadratic equation in T_d is obtained after some manipulations

$$T_d^2\omega_n^2-T_d\omega_n tg\Theta-\frac{1}{\beta}=0\,. \tag{11}$$

Expression for calculating T_d is the positive solution of (11)

$$T_d=\frac{tg\Theta}{2\omega_n}+\frac{1}{\omega_n}\sqrt{\frac{tg^2\Theta}{4}+\frac{1}{\beta}} \tag{12}$$

Hence, PID controller parameters are calculated using the expressions (10a), $T_i=\beta T_d$ and (12), where Θ is obtained from the phase condition (5)

$$\Theta=-180°+\phi_M-\arg G(\omega_n)=-180°+\phi_M-\varphi \tag{13}$$

Hence, using the designed PID controller, the identified point G of the plant frequency response $G(j\omega)$ with co-ordinates (3) is moved into the open-loop frequency response point L located on the unit circle M_1. Hence, the identified point G of the plant frequency response $G(j\omega)$ determines the gain crossover point L of the open-loop $L(j\omega)$

$$L\equiv L(j\omega_n)=\left[|L(j\omega_n)|,\arg L(\omega_n)\right]=\left[1,\phi_M\right] \tag{14}$$

for which the designed PID controller guarantees the required phase margin ϕ_M. Therefore for the excitation frequency ω_n $|L(j\omega_n)|=1$. Mutual situation of the points $G(j\omega_n)$ and $L(j\omega_n)$ is shown in Fig.3.

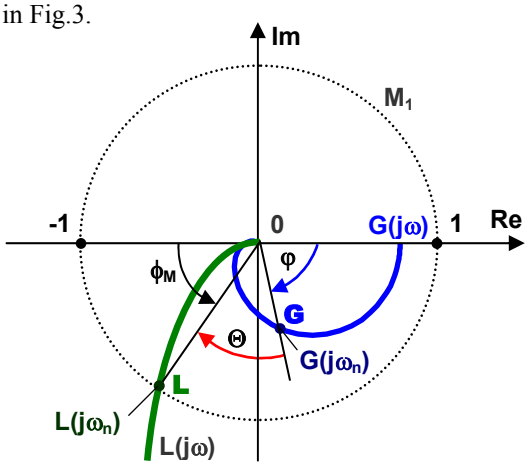

Fig.3. Graphical representation of the PID controller design in the complex plane

It is recommended to derive the frequency ω_n of the sinusoid from the plant ultimate frequency ω_c using the well-known relay experiment (Rotach, 1984), i.e. by switching SW in Fig.1 into „3". The excitation frequency is adjusted according to the empirical relation (Bucz and Kozáková, 2012)

$$\omega_n\in\langle 0.2\omega_c, 0.95\omega_c\rangle \tag{15}$$

How to transform the required maximum overshoot η_{max} and the settling time t_s into the couple of frequency-domain

parameters (ω_n, ϕ_M) needed for identification and PID controller coefficients tuning is described in the following subsection.

4. CLOSED-LOOP PERFORMANCE UNDER THE SINE-WAVE TYPE PID CONTROLLER

Looking for appropriate transformation $\Re:(\eta_{max}, t_s)\rightarrow(\omega_n, \phi_M)$, consider typical phase margins ϕ_M given by the set $(j=1...8)$

$$\phi_{Mj} = \{20°, 30°, 40°, 50°, 60°, 70°, 80°, 90°\} \qquad (16)$$

split into 5 equidistant sections $\Delta\omega_n=0,15\omega_c$, and generate the set of excitation frequencies $(k=1,\ldots,6)$

$$\omega_{nk} = \{(0.2, 0.35, 0.5, 0.65, 0.8, 0.95)\omega_c\} = \{\sigma_k \omega_c\} \qquad (17)$$

Each element in (17) represents a different identification level ω_{nk}. Fig.6 and Fig.7 show closed-loop step responses for plants

$$G_1(s) = \frac{1}{(s+1)^3}, \quad G_2(s) = \frac{e^{-0,5s}}{s+1} \qquad (18)$$

under PID controllers designed for three values of phase margin $\phi_M=40°, 60°, 80°$ on four different excitation levels $\sigma_1=\omega_{n1}/\omega_c=0,2$; $\sigma_2=\omega_{n2}/\omega_c=0,35$; $\sigma_3=\omega_{n3}/\omega_c=0,5$; and $\sigma_5=\omega_{n5}/\omega_c=0,8$, demonstrating qualitative effect of ω_{nk} and ϕ_{Mj} on closed-loop step response.

Achieving t_s and η_{max} was tested by designing PID controller for a vast set of benchmark examples (Åström and Hägglund, 2000) for excitation frequencies and phase margins expressed by Cartesian product $\phi_{Mj}\times\omega_{nk}$ of the sets (16) and (17) for $j=1,...,8$, $k=1,...,6$. Obtained dependences $\eta_{max}=f(\phi_M, \omega_n)$ and $t_s=(\phi_M, \omega_n)$ are plotted in Fig.4 (for non-integrating plants) and in Fig.5 (for integrating plants), where the relative settling time τ_s is t_s weighted by the plant ultimate frequency ω_c.

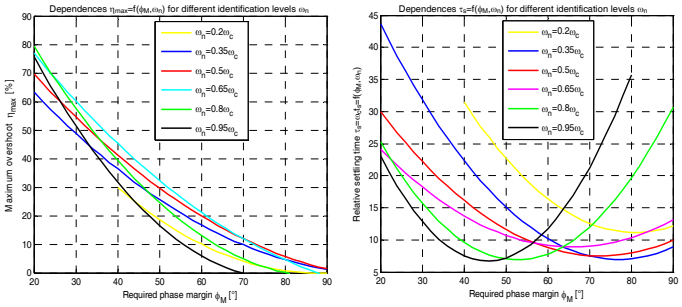

Fig.4. Dependences: a) $\eta_{max}=f(\phi_M, \omega_n)$, b) $\tau_s=\omega_c t_s=f(\phi_M, \omega_n)$ for controlled plants without integral behaviour, $\beta=T_i/T_d=4$

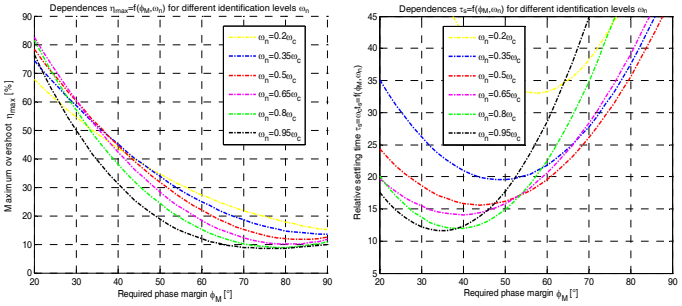

Fig.5. Dependences: a) $\eta_{max}=f(\phi_M, \omega_n)$, b) $\tau_s=\omega_c t_s=f(\phi_M, \omega_n)$ for controlled plants with integral behaviour, $\beta=T_i/T_d=12$

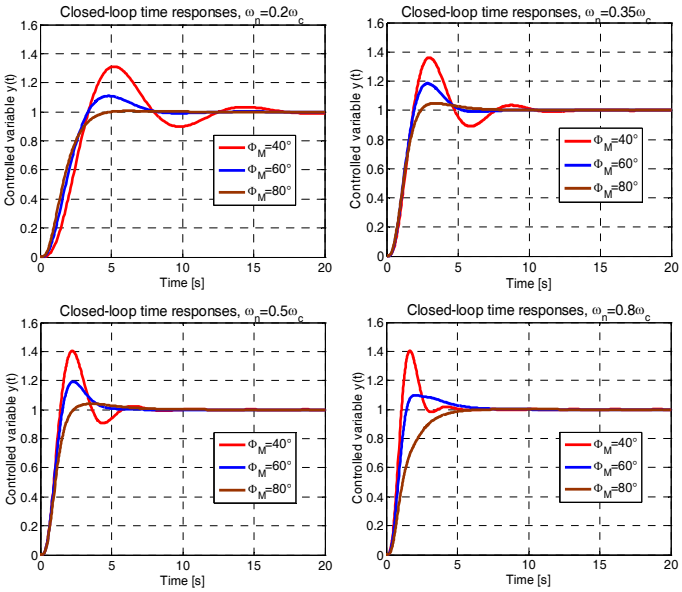

Fig.6. Closed-loop step responses of the plant $G_1(s)$ under PID controllers designed for various ϕ_M and ω_n

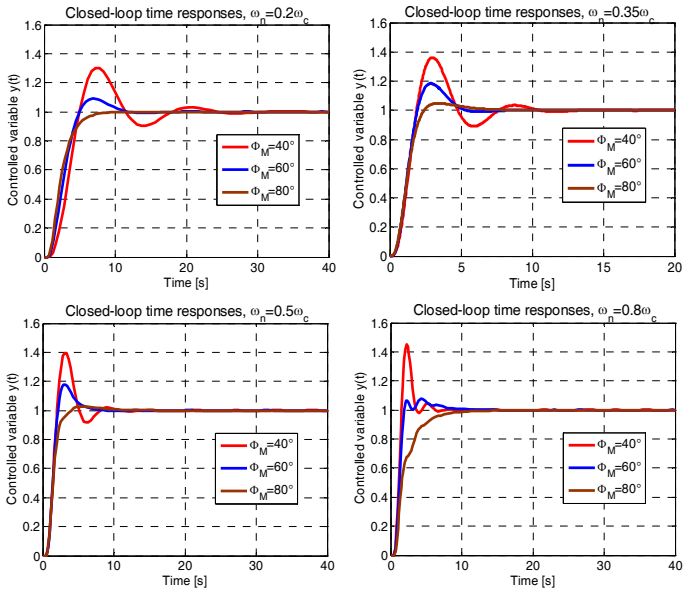

Fig.7. Closed-loop step responses of the plant $G_2(s)$ under PID controllers designed for various ϕ_M and ω_n

It is a well-known fact that the maximum overshoot η_{max} can be estimated from the desired phase margin ϕ_M, and similarly the settling time t_s can be estimated from the open-loop gain crossover frequency ω_a^*. According to Reinisch, analytical dependences $\eta_{max}=f(\phi_M)$ and $t_s=f(\omega_a^*)$ derived for second order closed-loop transfer functions are (Bucz and Kozáková, 2012)

$$\eta_{\max} = -0.91\phi_M + 64.55 \text{ for } \phi_M \in \langle 38°, 71° \rangle \qquad (19)$$

$$\eta_{\max} = -1.53\phi_M + 88.46 \text{ for } \phi_M \in \langle 12°, 38° \rangle \qquad (20)$$

$$\frac{\pi}{\omega_a^*} < t_s < \frac{4\pi}{\omega_a^*} \qquad (21)$$

The above Reinisch formulae are useful to express desired closed-loop dynamics in classical analytical design procedures.

However, with increased order of the closed-loop transfer function they fail to be valid, and are not applicable in tuning methods if the mathematical model of the plant is unknown. Let us express the closed-loop settling time t_s similarly as in (21)

$$t_s = \frac{\gamma\pi}{\omega_n} \tag{22}$$

where γ represents the shape factor of the closed-loop step response. In the Reinisch relation for a 2nd order closed-loop system its value usually ranges from 1 to 4, depending on damping coefficient specifications (Bucz and Kozáková, 2012). In the proposed sine-wave method, γ changes more considerably within the interval (0.5;16) strongly depending on the phase margin ϕ_M at the given excitation frequency ω_n.

To explore settling times of closed-loops with different dynamics it is useful to define a new performance measure, the so-called relative settling time

$$t_s\omega_n = \pi\gamma(\phi_M) \tag{23}$$

Substituting for $\omega_n=\sigma\omega_c$ into (23) we can define the relative settling time $\tau_s=t_s\omega_c$ as follows

$$t_s\omega_c = \frac{\pi}{\sigma}\gamma(\phi_M) \tag{24}$$

The relative settling time (24) relates the settling time t_s with the plant ultimate frequency ω_c, whereby the left-hand side of (24) is independent from the excitation frequency ω_n. This empirical dependence is plotted in Fig.4b (for non-integrating plants) and Fig.5b (for integrating plants) for different identification levels ω_{nk}, showing that with increasing the desired phase margin ϕ_M, the relative settling time first drops and after achieving its optimal value τ_{s_opt} grows again quadratically.

Empirical dependences in Fig.4 and Fig.5 have been approximated by quadratic regression curves and are called B-parabolas (Bucz and Kozáková, 2012). B-parabolas are a useful tool to carry out the transformation $\Re:(\eta_{max},t_s)\rightarrow(\omega_n,\phi_M)$ that enables to choose appropriate values of phase margin and excitation frequency ϕ_M and ω_n, respectively, to guarantee the performance specified in terms of maximum overshoot η_{max} and settling time t_s.

Note that pairs of B-parabolas at the same level are always to be used.

The sine-wave type PID controller design procedure

1. Set the PID control into manual mode. Find the critical frequency ω_c of the plant using the multipurpose loop in Fig.1 (SW in position „3“).
2. From the required settling time t_s calculate the relative settling time $\tau_s=\omega_c t_s$.
3. On the vertical axis of the plot in Fig.4b or Fig.5b find the value τ_s calculated in Step 2.
4. Choose the excitation level σ (e.g. $\sigma_5=\omega_{n5}/\omega_c=0,8$).
5. For τ_s, find the corresponding phase margin ϕ_M on the parabola $\tau_s=f(\phi_M,\omega_n)$ at excitation level found in Step 4.
6. Read ϕ_M from Step 5 on the horizontal axis of the plot in Fig.4a or Fig.5a, and find the corresponding maximum overshoot η_{max} on the parabola $\eta_{max}=f(\phi_M,\omega_n)$ at the excitation level found in Step 4.
7. If the found η_{max} is inappropriate, repeat steps 4 to 6 for parabolas $\tau_s=f(\phi_M,\omega_n)$, and $\eta_{max}=f(\phi_M,\omega_n)$ corresponding to other levels $\sigma_k=\omega_{nk}/\omega_c$ (related with the choice $\sigma_5=\omega_{n5}/\omega_c=0,8$ for $\sigma_k=\{0,2;0,35;0,50;0,65;0,95\}$, $k=1...4,6$). Repeat until both required performance measures η_{max} and t_s are satisfied.
8. Using the critical frequency ω_c (from Step 1) and the chosen excitation level σ (from Step 4), calculate the excitation frequency ω_n according to $\omega_n=\sigma\omega_c$.
9. Identify the plant using sinusoidal excitation signal with frequency ω_n specified in Step 8 (SW is in position „2“).
10. Specify $\varphi=argG(\omega_n)$, and $|G(\omega_n)|$. Calculate the controller argument Θ by substituting φ and ϕ_M into (13).
11. Calculate the PID controller parameters by substituting the identified values $\varphi=argG(\omega_n)$, $|G(\omega_n)|$ and specified ϕ_M into tuning rules (10a), $T_i=\beta T_d$ and (12).

The above PID controller design procedure has been integrated into the auto-tuning algorithm of the presented sine-wave method. To estimate computation time t_h of PID coefficients, following approximate relation can be used

$$t_h = t_{3-7} + (2...4)\left[\frac{2\pi}{\omega_c} + \frac{1}{\omega_n}\right] \tag{25}$$

where t_{3-7} is convergence time of the iteration fragment (steps 3…7 of the above procedure). It is evident, that computation time of PID coefficients depends on the plant dynamics.

5. VERIFICATION OF THE SINE-WAVE METHOD ON BENCHMARK EXAMPLES

Using the sine-wave method let us design ideal PID controllers (6) for the following plants

$$G_A(s) = \frac{1}{(0,01s+1)^3},\ G_B(s) = \frac{1,3}{s(7,51s+1)}e^{-2,1s} \tag{26}$$

The control objective is to secure two different performances:

- $(\eta_{max1},\tau_s)=(30\%,12)$; $(\eta_{max2},\tau_s)=(5\%,12)$ for the plant G_A,
- $(\eta_{max1},\tau_s)=(30\%,20)$; $(\eta_{max2},\tau_s)=(20\%,20)$ for the plant G_B.

PID controller design for the plant $G_A(s)$

Critical frequency of the plant identified by the Rotach test is $\omega_c=173,216[rad/s]$. The prescribed closed-loop settling time is $t_s=\tau_s/\omega_c=12/173,216[s]=69,3[ms]$.

For the *first expected performance* $(\eta_{max1};\tau_s)=(30\%;12)$ a satisfactory choice is $(\phi_{M1};\omega_{n1})=(50°;0,5\omega_c)$ resulting from the $B_{0,5}$ parabola in Fig.4. *The second performance in terms of* $(\eta_{max2};\tau_s)=(5\%;12)$ can be achieved by choosing $(\phi_{M2};\omega_{n2})=(70°;0,8\omega_c)$ resulting from the $B_{0,8}$ parabola in Fig.4. Sine-wave type identification of $G_A(s)$ at excitation frequencies $\omega_{n1}=0,5\omega_c$ and $\omega_{n2}=0,8\omega_c$ is depicted in Fig.8.

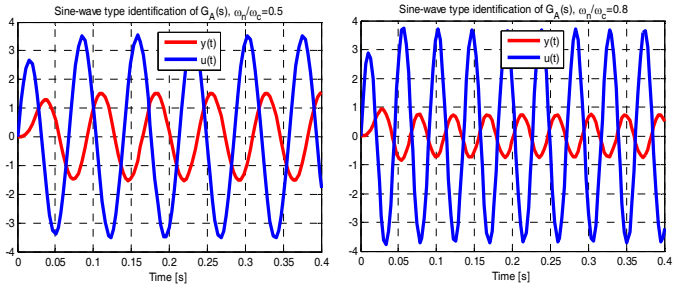

Fig.8. Sine-wave type identification of the plant $G_A(s)$ at
a) $\omega_{n1}/\omega_c=0,5$ for $(\eta_{max1},\tau_s)=(30\%,12)$;
b) $\omega_{n2}/\omega_c=0,8$ for $(\eta_{max2},\tau_s)=(5\%,12)$

Identified points for the first and second designs are $G_A(j0,5\omega_c)=0,43e^{-j120^\circ}$ and $G_A(j0,8\omega_c)=0,19e^{-j165^\circ}$, respectively. According to Fig.9, both points are located in the Quadrant II of the complex plane, on the Nyquist plot $G_A(j\omega)$ (blue curve in Fig.9) which verifies the identification.

Using the PID controller designed for $(\phi_{M1};\omega_{n1})=(50^\circ;0,5\omega_c)$, the point $G_A(j0,5\omega_c)$ is moved into the gain crossover $L_{A1}(j0,5\omega_c)=1e^{-j130^\circ}$ on the unit circle M_1, which verifies achieving the phase margin $\phi_{M1}=180^\circ-130^\circ=50^\circ$ (red Nyquist plot in Fig.9). By designing PID controller for $(\phi_{M2};\omega_{n2})=(80^\circ;0,8\omega_c)$, the point $G_A(j0,8\omega_c)$ has been moved into $L_{A2}(j0,8\omega_c)=1e^{-j110^\circ}$ yielding phase margin $\phi_{M2}=180^\circ-110^\circ=70^\circ$ (green Nyquist plot in Fig.9).

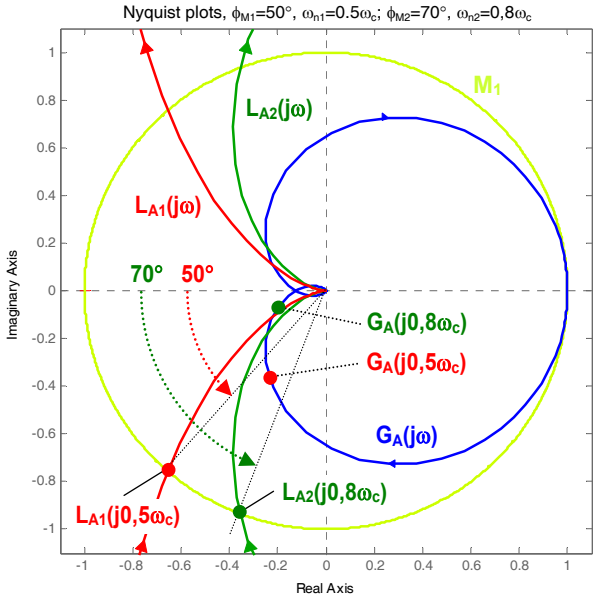

Fig.9. Nyquist plots of $G_A(s)$, and open-loops for required performances $(\eta_{max1},\tau_s)=(30\%,12)$ and $(\eta_{max2},\tau_s)=(5\%,12)$

Performance read from the closed-loop step response in Fig.10b (red plot) $\eta_{max1}^*=29,7\%$, $t_{s1}^*=58,4[ms]$ was achieved using PID controller coefficients $(K;T_i;T_d)=(2.2811;0.0194;0.0049)$. Performance in terms of $\eta_{max2}^*=4,89\%$, $t_{s2}^*=60,5[ms]$ identified from the closed-loop step response in Fig.10a (green plot) complies with the required performance. In this case the PID controller parameters are $(K;T_i;T_d)=(2.9826;0.0488;0.0122)$.

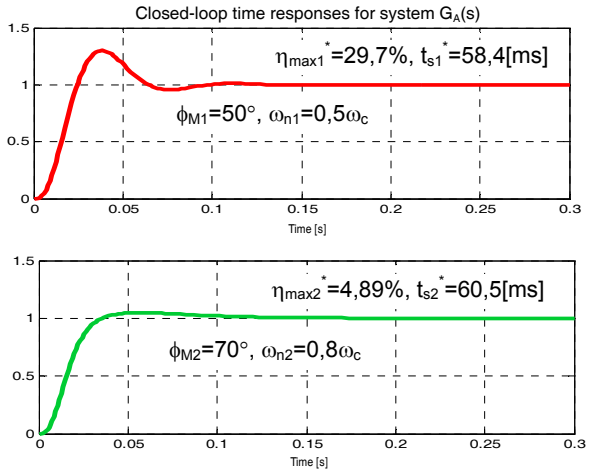

Fig.10. Closed-loop step responses with $G_A(s)$ and required performance a) $(\eta_{max1},\tau_s)=(30\%,12)$, b) $(\eta_{max2},\tau_s)=(5\%,12)$

PID controller design for the plant $G_B(s)$

According to plant critical frequency $\omega_c=0,2407[rad/s]$, the required settling time is $t_s=\tau_s/\omega_c=20/0,2407[s]=83,09[s]$. Time delay of $G_B(s)$ is $D_B=2,1[s]$.

The *first performance specification* $(\eta_{max1};\tau_s)=(30\%;20)$ can be provided using the $B_{0,35}$ parabolas for $\beta=12$ (Fig.5) at $\omega_{n1}/\omega_c=0,35$ and for parameters $(\phi_{M1};\omega_{n1})=(53^\circ;0,35\omega_c)$, supplying the augmented open-loop phase margin $\phi_{M1}'=\phi_{M1}+\omega_{n1}D_B=53^\circ+10,1^\circ=63,1^\circ$ into the controller design algorithm. The *second performance specification* $(\eta_{max2};\tau_s)=(20\%,20)$ is achievable using the $B_{0,5}$ parabolas in Fig.5 for $\beta=12$ and $\omega_{n2}/\omega_c=0,5$ and parameters $(\phi_{M2};\omega_{n2})=(62^\circ;0,5\omega_c)$. To reject the influence of D_B, instead of $\phi_{M2}=62^\circ$ the augmented open-loop phase margin $\phi_{M2}'=\phi_{M2}+\omega_{n2}D_B=62^\circ+14,5^\circ=76,5^\circ$ was supplied into the PID controller design algorithm. Sine-wave type identification of $G_B(s)$ at $\omega_{n1}=0,35\omega_c$ and $\omega_{n2}=0,5\omega_c$ is depicted in Fig.11.

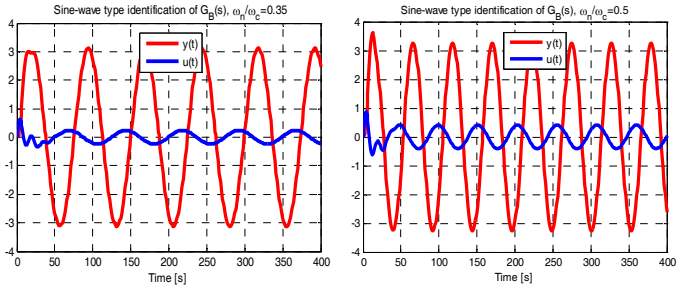

Fig.11. Sine-wave type identification of the plant $G_B(s)$ at
a) $\omega_{n1}/\omega_c=0,35$ for $(\eta_{max1},\tau_s)=(30\%,20)$;
b) $\omega_{n2}/\omega_c=0,5$ for $(\eta_{max2},\tau_s)=(20\%,20)$

Using PID controller, the first identified point $G_B(j0,35\omega_c)=12,7e^{-j122^\circ}$ (Design No.1) was moved into the gain crossover $L_{B1}(j0,35\omega_c)=1e^{-j127}$ located on the unit circle M_1; this verifies achieving the phase margin $\phi_{M1}=180^\circ-127^\circ=53^\circ$ (red Nyquist plot in Fig.12). Achieved performance $(\eta_{max1}^*=29,6\%, t_{s1}^*=81,73[s])$ red from the closed-loop step response in Fig.13a (red plot) was obtained using designed controller coefficients $(K;T_i;T_d)=(0.0783;26.2993;6.5748)$.

The second identified point $G_B(j0,5\omega_c)=8,10e^{-j129°}$ (Design No.2) was moved into $L_{B2}(j0,5\omega_c)=1e^{-j118°}$ achieving the phase margin $\phi_{M2}=180°-118°=62°$ (green Nyquist plot in Fig.12). Achieved performance ($\eta_{max2}^*=19,7\%$, $t_{s2}^*=82,44[s]$) red from the step response in Fig.13b (green plot) meets the required specification and was obtained by PID controller with coefficients (K;T_i;T_d)=(0.1090;14.2784;3.5696).

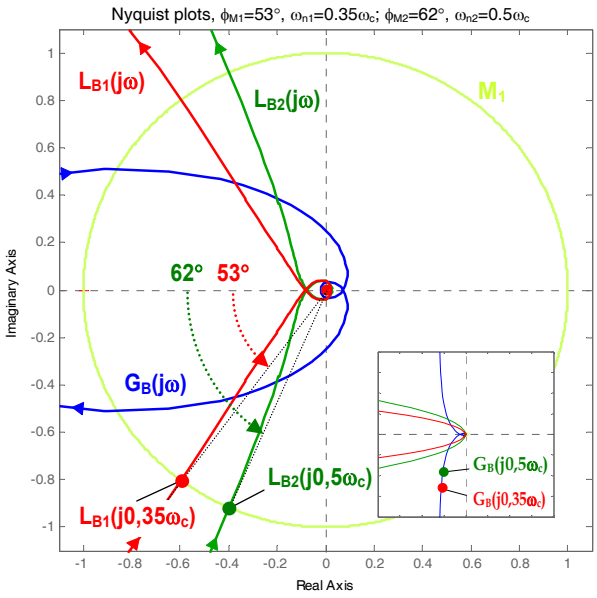

Fig.12. Nyquist plots of $G_B(s)$, and open-loops for required performances $(\eta_{max1},\tau_s)=(30\%,20)$ and $(\eta_{max2},\tau_s)=(20\%,20)$

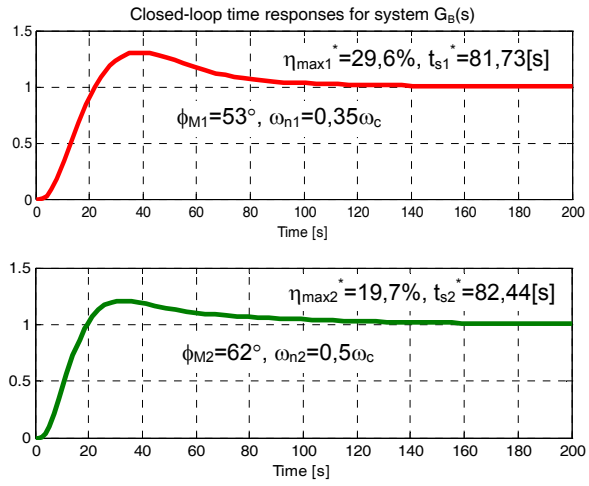

Fig.13. Closed-loop step responses with $G_B(s)$, and required performance a) $(\eta_{max1},\tau_s)=(30\%,20)$, b) $(\eta_{max2},\tau_s)=(20\%,20)$

6. VERIFICATION OF THE SINE-WAVE METHOD ON A REAL PLANT

The sine wave method was applied to control a physical model of a DC permanent magnet motor; controlled variable was the speed, and plant input u(t) was armature voltage generated using the Matlab-Realtime Workshop control system. A speed-voltage generator was used to sense the output variable y(t). The control objective was to guarantee the performance requirements: $\eta_{max1}=10\%$, $\eta_{max2}=25\%$ and $\tau_s=10$.

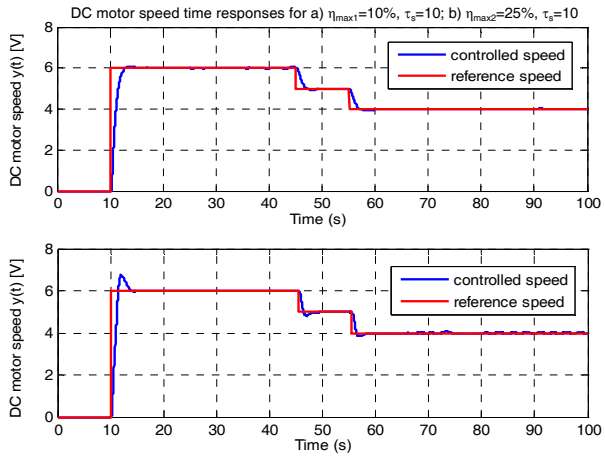

Fig.14. Closed-loop time responses of the DC motor speed for a) $\eta_{max1}=10\%$, $\tau_s=10$; b) $\eta_{max2}=25\%$, $\tau_s=10$

7. CONCLUSIONS

Resulting closed-loop step responses depicted in Fig.10, Fig.13 and Fig.14 prove that PID controllers were able to guarantee the required performance measure values. The proposed new sine-wave type design method allows successful PID controller tuning. Another important contribution of the paper is construction of empirical plots converting engineering time-domain requirements specified by a process technologist (maximum overshoot and settling time) into frequency domain performance specification (in terms of phase margin and gain crossover frequency).

ACKNOWLEDGMENT

This research work has been supported by the Scientific Grant Agency of the Ministry of Education of the Slovak Republic, Grant No. 1/1241/12.

REFERENCES

Åström, K.J. and Hägglund, T. (2000). Benchmark Systems for PID Control. *IFAC Workshop on Digital Control PID'00,* pp. 181-182, Terrassa, Spain, April 5-7, 2000.

Bucz, Š. and Kozáková, A. (2012). PID Controller Design for Specified Performance. *Introduction to PID Controllers: Theory, Tuning and application to frontier areas.* Department of Chemical Engineering, CLRI, Adyar, Chennai, India, 2012, ISBN 978-953-307-927-1.

Kozáková, A., Veselý, V. and Osuský, J. (2010). Decentralized Digital PID Design for Performance. *In: 12th IFAC Symposium on Large Scale Systems: Theory and Applications,* Lille, France, 12.-14.7.2010, Ecole Centrale de Lille, ISBN 978-2-915-913-26-2.

Osuský, J.; Veselý, V. and Kozáková, A. (2010). Robust decentralized controller design with performance specification, *ICIC Express Letters,* Vol. 4, No. 1, pp. 71-76, ISSN 1881-803X, Kumamoto, Japan.

Rotach, V. (1984). Avtomatizacija nastrojki system upravlenija. *Energoatomizdat,* Moskva, (in Russian)

Veselý, V. (2003). Easy Tuning of PID Controller. *Journal of Electrical Engineering,* Vol.54, No.5-6, pp. 136-139, ISSN 1335-3632, Bratislava, Slovak Republic.